Comparission between 6 Blade and 20 Blade Impeller by Using CFD Analysis

Suresh Pittala

School of Mechanical and Industrial Engineering

Hawassa University, Post Box No-5, Hawassa, Ethiopia.

Abstract

Designing impellers for pump are important for fluid flow analysis. Six blade impellers are commonly used in the industries presently. In this paper we have proposed 20 blade impeller, in order to reduce cost and noise. Also Comparission between these impellers are made in respect to other aspects like material, outlet velocity, fluid discharge and efficiency. By using computational fluid dynamics (CFD).To improve the efficiency of pump, CFD analysis is one which is used in the pump industry.For 6 blade impeller used material is steel and 20 blade impeller material isAcrylonitrile butadiene styrene (ABS)which is used to reduce noise and cutting down the cost of the impeller. The number of impeller blades is proposed to increase from 6-8 to 20 in order to increase fluid velocity. Inlet blade angle is reduced to less than 40 degrees from greater than 45 degrees in order not only to increase efficiency but also outlet fluid velocity of the impeller in case of 20 blade. In the first case outlet angle is increased, and in the second case inlet angle is decreased and they are obtained from the CFD analysis andit causes to improve efficiency of 20 blade impeller. By changing the outlet angle the head of the impeller is improved when compared with 6 blade impeller. Further, from CFD analysis the calculated efficiency of the impeller with optimum vane head created by this analysis would be higher in 20 blade impeller.

KEY WORDS:Computational Fluid Dynamics (CFD) analysis, 6 blade Impeller, 20 blade impeller, pump.

1. Introduction

A wide variety of centrifugal pump types have been constructed and used in many different applications in industry and other technical sectors. However, their design and performance

prediction process is still a difficult task, mainly due to the great number of free geometric parameters; the effect of these cannot be directly evaluated. The significant cost and time of the trial-and-error process by constructing and testing physical prototypes reduces the profit margins of the pump manufacturers. For this reason CFD analysis is currently being used in the design and construction stage of various pump types. The experimental way of pump test can give the actual value of head developed, power rating and efficiency. But the internal flow conditions cannot be predicted by the experimental results. From the CFD analysis software and advanced post processing tools the complex flow inside the impeller can be analyzed. The complex flow characteristics like inlet pre-swirl, flow separation and outlet recirculation cannot be visualized by the experimental way of pump test. But in the case of CFD analysis the above flow characters can be visualized clearly.

Computational fluid dynamics (CFD) analysis is being increasingly applied in the design of centrifugal pumps. With the aid of the CFD approach, the complex internal flows in water pump impellers, which are not fully understood yet, can be well predicted, to speed up the pump design procedure. Thus, CFD is any important tool for pump designers. The use of CFD tools in turbo machinery industry is quite common today. Many tasks can numerically be solved much faster and cheaper than by means of experiments. Nevertheless the highly unsteady flow in turbo machinery raises the question of the most appropriate method for modelling the rotation of the impeller.CFD analysis is very useful for predicting pump performance at various mass-flow rates. For designers, prediction of operating characteristics curve is most important. All theoretical methods for prediction of Efficiency merely give a value; but one is unable to determine the root cause for the poor performance.

The purpose of the 6 blade impeller is to show a numerical study of a centrifugal pump impeller taking into account the whole 3-D geometry and the unsteadiness of the flow. It has been done with the commercial software package CFD. Code uses the finite volume method and solves the k-ε equations with ability to handle unstructured grids, include relative reference frames and make unsteady calculations with moving meshes [1].

Impellers are prevalent for much different application in the industrial or other sector. Nevertheless, their design and performance prediction process is still a difficult task mainly due to the great number of free geometric parameters, the effect of which cannot be

directly evaluated. The significant cost and time of the trial and error process by manufacturing and testing of physical prototype reduces the profit margins of the impeller manufacturers. For this reason CFD analysis is currently used in hydrodynamic design for different impeller types. Impeller is a rotating part of a centrifugal compressor/pump that imparts kinetic energy to a fluid. Here under we introduced (1) modeling laws and (2) Vibration and noise [2].

Modeling Laws The modeling laws includes both the affinity law and model law. These two laws are stated as,Affinity Law "for similar conditions of flow the capacity will vary directly with the ratio of speed and/or impeller diameter and the head with the square of this ratio at the point of best efficiency".Model Law **"**two geometrically similar pumps working against the same head will have similar flow conditions if they run at speeds inversely proportional to their size, and in that case their capacity will vary with the square of their size".

According to Bernoulli the differential pressure equation is given by

$$\frac{P_1}{\rho}+\frac{V_1^2}{2}+Z_1 g=\frac{P_2}{\rho}+\frac{V_2}{2}+Z_2 g \qquad (1)$$

$V_2 = 0;$ $Z_1 = Z_2.$

The difference pressure equation is given by

$$(P_2-P_1)=\frac{V^2*\rho}{2} \qquad (2)$$

Where

P_1 =Initial pressure at the inlet of the impeller, in bar

P_2 = Final pressure at the outlet of the impeller, in bar

ρ = Density of air in kg/m^3

V =Velocity of air in m/s

2. **Governing equations**

CFD applies numerical methods called discretization to develop approximations of the governing equations of fluid mechanics and the fluid region to be studied. The set of approximating equations are solved numerically for the flow field variables at each node [3].

$$\frac{\partial}{\partial t}\int_{v} \rho\, \emptyset dv + \oint_{A} \rho \emptyset V \,.\, dA \;=\; \oint_{A} \Gamma \nabla \emptyset \,.\, dA + \int_{V} s_{\emptyset}\, dV$$

<Unsteady> + <Convention> = <Diffusion> + <Generation>

Fig 1: General conversation

To keep the details simple, we illustrate the fundamental ideas underlying CFD by applying them to the following simple first order differential equation:

$$\frac{du}{dx} + u_m = 0; 0 \le x \le 1; u(0) = 1 \qquad (3)$$

It first considers the case where m = 1 when the equation is linear. This later considers the case where m= 2 when the equation is nonlinear. This derives a discrete representation of the above equation with m = 1 on the following grid:

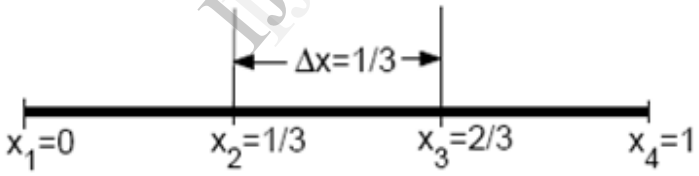

This grid has four equally-spaced grid points with Δx being the spacing between successive points. Since the governing equation is valid at any grid point, we have

$$\left[\frac{du}{dx}\right]_i + u_i = 0. \qquad (4)$$

Here the subscript i represents the value at grid point x_i . In order to get an expression for $(du/dx)_i$ in terms of u at the grid points, we expand u_{i-1} in a Taylor's series as

$$u_{i-1} = u_i - \Delta x \left[\frac{du}{dx}\right] + o(\Delta x^2). \qquad (5)$$

A simple rearrangement of (5) gives

$$\left[\frac{du}{dx}\right]_i = \frac{u_i - u_{i-1}}{\Delta x} + o(\Delta x). \qquad (6)$$

The error in $(du/dx)_i$, due to the neglected terms in the Taylor's series, is called the truncation error. Since the truncation error is $O(\Delta x)$, this discrete representation is termed first order accurate. Using (6) in (5) and excluding higher-order terms in the Taylor's series, we get the discrete equation as [4]

$$\frac{u_i - u_{i-1}}{\Delta x} + u_i = 0 \ . \qquad (7)$$

This method of deriving the discrete equation using Taylor's series expansions is called the finite-difference method. However, most commercial CFD codes use the finite-volume or finite-element methods which are better suited for modeling flow past complex [5].

3. CFD Procedure and Analysis

Fluid flow analysis performed on the impeller, using ANSYS CFX. Numerical results fully characterized the flow field, providing detailed flow information such as flow speed, flow angle, pressure, boundary layer development, losses [6]. The flow field information from CFD simulation was then used to help elucidate the flow physics. Impeller, blade geometry is shown in fig2.Design specification of 6 blade and 20 blade impellers are shown in table 1 and table 2.

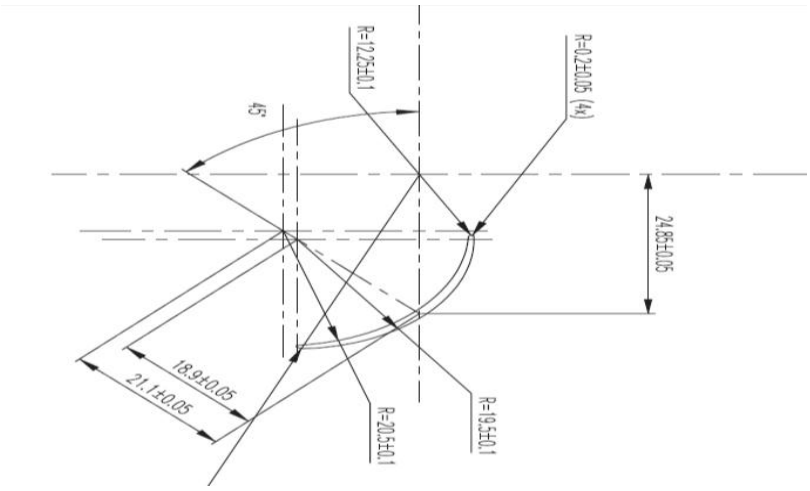

Fig.2. Blade geometry of 20 blade impeller

S.no	Parameter	6 blade impeller	20 blade impeller
1	Inlet diameter (D_i)	52 mm	22.67 mm
2	Outlet diameter(D_0)	111 mm	67.74 mm
3	Blade number	6	20
4	Inlet angle (α)	73.5^0	38^o
5	Outlet angle (β)	56.5^0	62^0
6	Blade thickness (t)	3mm	2.5 mm
7	Shaft diameter (D_s)	14 mm	6 mm

Tables 1: Design Specification of 6 blade Impeller and 20 blade impeller

3.1 Meshing of impeller blades

Turbo grid uses unstructured meshes in order to reduce the amount of time spent generating meshes. The geometry modeling and mesh generation process simplifying model more complex geometries that can be handled with conventional Multi-block structured meshes. The mesh is adapted to resolve the flow-field features [7]. This flexibility allows picking mesh topologies that are best suited for particular application. The geometry is created by using Solid Works and the extruded geometry is meshed by Turbo Grid. Meshing 20 blades Impeller is shown in fig. 3.Mesh statistics and comparison between 6 blade and 20 blade is shown in tab.2, tab.3 and tab.4.

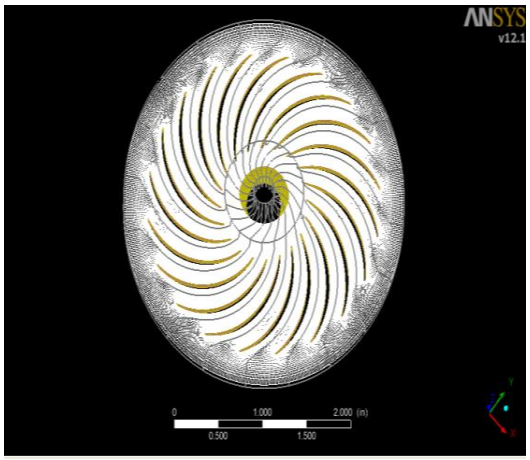

Fig.3. Meshing of 2o Blade impeller

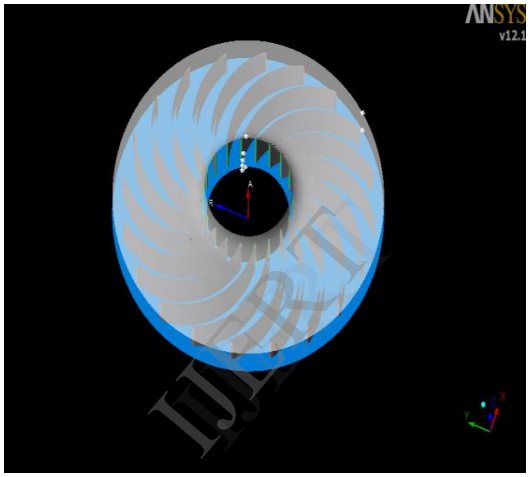

Fig.4. 20 blades Impeller

S. No.	Mesh measure	Value
1.	Minimum face angle	26.2748
2.	Maximum face angle	153.725
3.	Maximum element	382,072
4.	Minimum volume	1,74683e-012[inches]
5.	Maximum edge	1970.8

Table.2. Mesh Statistics of 20 blade impeller

No. of Nodes	111637
No. of Elements	149456

Table.3: Mesh statistics 6 blade impeller

S. No.	Parameter	6 blade impeller	20 blade impeller	Benefits of New model
1	Inlet angle	73.5^0	38^0	Flow increment
2	Outlet angle	56.5^0	62^0	Flow increment
3	Number of blades	6	20	Flow increment
4	Material	Steel	ABS (C_8H_8)	Cost reduction
5	Outlet velocity	23.22 m/s	32.46 m/s	Outlet velocity increment
6	Discharge	4.00 Lps	5.2 Lps	Discharge increased
7	Head	12 m	18 m	Head Increased

Table.4. Comparisons between 6 blade and 20 blade impeller

3.2 CFX Preprocessor

Centrifugal pump impeller domain is considered as rotating frame of reference with different rotational speed of 10000RPM, 8000RPM, 6000 rpm, 4000 rpm, and 2000 rpm. The working fluid through the pump is water at 300k. K-ε turbulence model. Inlet static pressure and outlet mass flow rate 29.63 kg/mol. Three dimensional incompressible N-S equations are solved with ANSYS-CFX Solver (for 20 blade impeller) [8].

Centrifugal pump impeller domain is considered as rotating frame of reference with different rotational speed of 2842RPM, 2848RPM, 2858 rpm, 2866 rpm, and 2918 rpm [9]. The working fluid through the pump is water at 300k. K-ε turbulence model. Inlet static pressure and outlet different mass flow rate of 8.78 kg/s,6.83 kg/s, 6.25 kg/s,5.30 kg/s,0.00 kg/s are given as boundary conditions [10]. Three dimensional incompressible N-S equations are solved with ANSYS-CFX Solver(for 6 blade impeller).

3.2.1 Wall Boundary Conditions No-slip conditions were prescribed on the impeller blade surface. Zero Neumann boundary condition was imposed for pressure at the walls [11].

3.3 CFX Postprocessor

In this we can view the results such as contours, vectors and streamlines. In the results velocity contour, total pressure and pressure contours are shown.

4. Results and Discussion

4.1 Span wise Velocity contours at 10000 rpm at 20 %, 50% and 70% for 20 blade impeller.

As Sean from figures 5 to 6, the velocity distribution varies as the speed of the impeller changes. Figure 7 represents high velocity (32.46 m/s).the flow separation takes place at middle of the blade from inlet compare to 10000 rpm the flow separation takes place at the end of the blade. From the above figures tells if the speed of the impeller increases automatically velocity also increase.

Fig5: velocity contour 20% at 10000 rpm

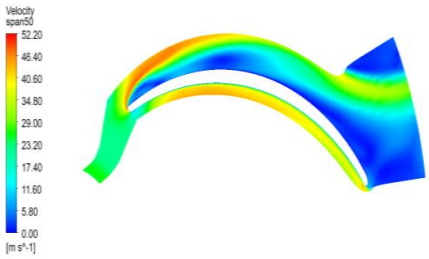

Fig6: velocity contour 50% at 10000 rpm

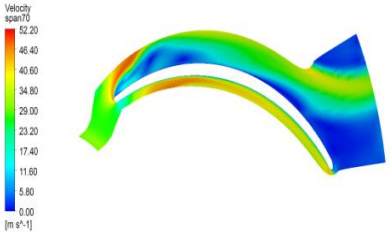

Fig7: velocity contour 70% at 10000 rpm

4.2 Static Pressure contours at 10000 rpm,at 20 %, 50% and 70% for 20 blade impeller.

As Sean in the figures the pressure distribution will varies as the speed of the impeller changes. From figure 10 the pressure at inlet is as compared to the pressure at outlet in 10000rpm case but in the 2000 rpm case the pressure at inlet is low and the pressure at outlet is high that means the exit velocity in 2000 rpm is low as compared to 10000rpm.

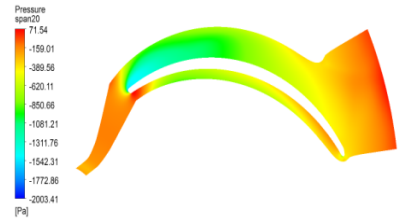

Fig8: static pressure contour 20% at 10000 rpm

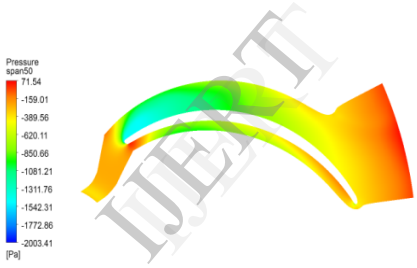

Fig9: static pressure contour 50% at 10000 rpm

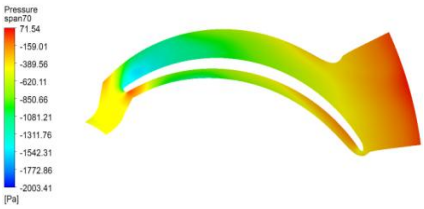

Fig10: static pressure contour 70% at 10000 rpm

4.3 Total Pressure contours at 10000 rpm at 20%, 50 % and 70% for 20 blade impeller.

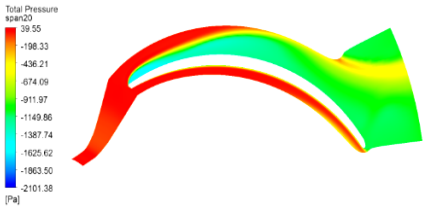

Fig11: Total Pressure Contour 20% at 10000 rpm

Fig12: Total Pressure 50% at 10000 rpm

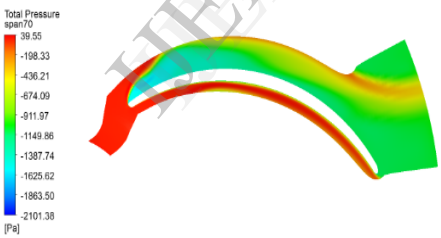

Fig13: Total Pressure Contour 70% at 10000 rpm

4.4 Span wise velocity Profiles at 10000 rpm, 8000 rpm, 6000 rpm, 4000 rpm and 2000

Profiles of span wise velocity component are shown in Figs for 10000 rpm, 8000 rpm, 6000 rpm, 4000 rpm and 2000 rpm respectively. The figures X axis represents axial chord and Y axis represents velocity in m/s. the figure represents flow variations in 10000rpm, 20%, 50%, 70% span wise.

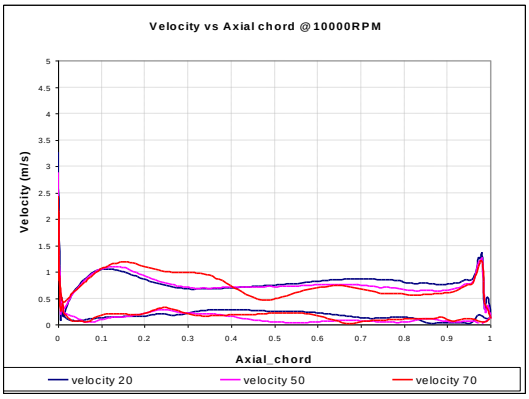

Fig. 14: Velocity and static pressure contours at 20%, 50% and 70% at 10000 rpm

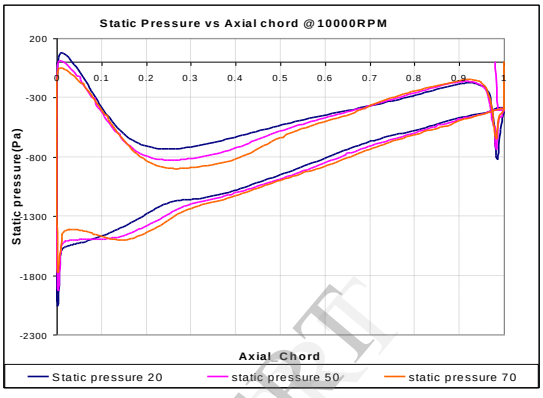

Fig. 15: Velocity and static pressure contours at 20%, 50% and 70% at 10000 rpm

Mean contours of span wise pressure component are shown in Fig 15 for 10000 rpm. The figure X axis represents axial chord and Y axis represents pressure in Pa. the figure 15 represents flow variations in 10000 rpm at contours 20%, 50%, 70% span wise.

4.5 Mean Span wise total pressure profiles for 20 blade impeller

Mean contours of span wise total pressure component are shown in Figs for 10000 rpm , 8000 rpm, 6000 rpm, 4000 rpm and 2000 rpm respectively. The figures X axis represents axial chord and Y axis represents total pressure in Pa. the figures represents flow variations in 10000 rpm , 8000 rpm , 6000 rpm , 4000 rpm and 2000 rpm at contours 20% , 50%, 70% span wise at outlet.

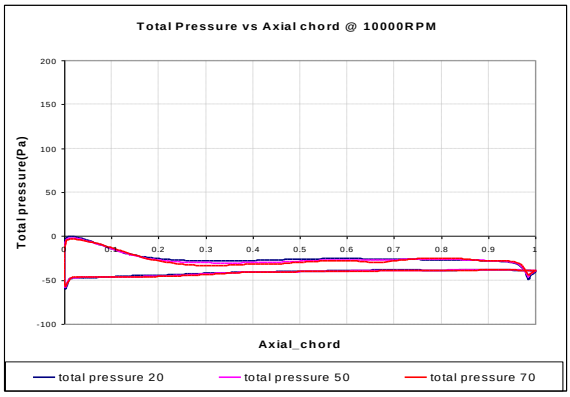

Fig.16: Total Pressure at 20%, 50% and 70% at 10000 rpm& Rpm vs Mass flow rate

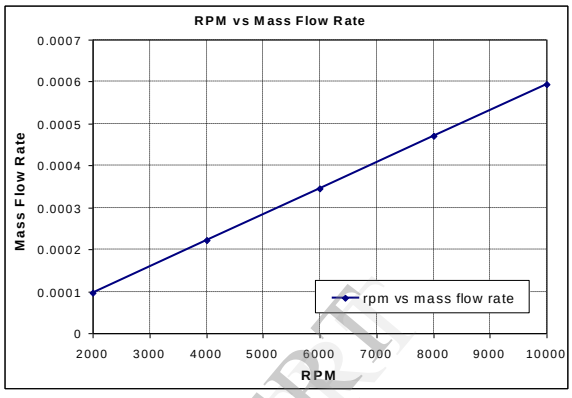

Fig.17: Total Pressure at 20%, 50% and 70% at 10000 rpm& Rpm vs Mass flow rate

From figure 17 shows at different rpms (10000, 8000, 6000, 4000 and 2000) the behavior of fluid flow at outlet. If the rpm increases the flow at outlet will also increases.

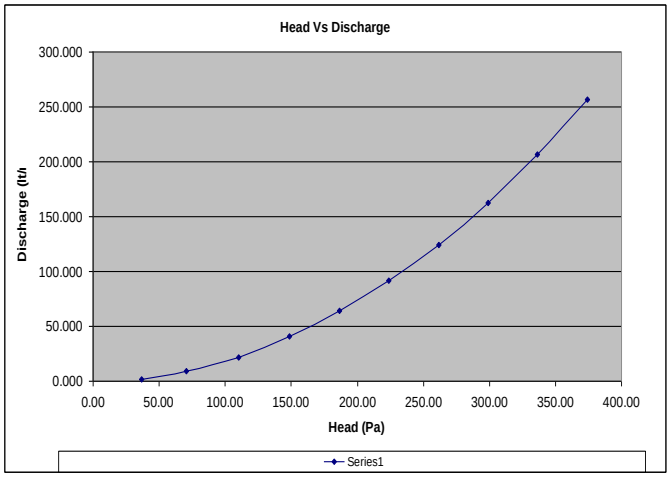

Fig.18: Head vs Discharge for 20 blade impeller

The graph shows head vs discharge-axis represents head in Pa and Y-axis represents discharge in m^3 /s. The above graph shows there is no formation of surge and stall.

5. Conclusions and Scope

The proposed improvements include (a) Impeller & blade material to be changed (b) Number of blade increases (c) Blade inlet angle to be changed (d) Blade outlet angle to be changed (e) CFD software results compare with the classical and new model.

Compared to 6 blade and 20 blade impeller, 20 blade impeller gives more discharge at the outlet of the impeller and also velocity obtained from the CFD predictions is 35.46 m/s. It has been observed that compared to these impellers 20 blade impeller is free from surge and stall. There is no formation of wake in 20 blade impeller. It has been observed that velocity of the fluid is directly proportional to impeller's RPM. Correlation has been derived between Head and Discharge. Correlation has been derived between RPM and Mass flow rate.

Future work should involve advancing the solution further in time for dynamic inflow or outflow boundary condition; and all the present simulations may be performed on a finer grid. Grid refinement may be done in order to obtain accurate results in both span wise as well as pitch wise direction.

6. Reference

[1]. Baun D.O., Flack R.D. 2003. Effects of volute design and number of impeller blades on Lateral impeller forces and hydraulic performance, International Journal of Rotating Machinery, Vol. 2, No. 9, pp. 145-152.

[2]. Labanoff Robert R. Ross,Centrifugal blower impeller design & application Gulf Publishing Company, Houston, TX, 1992, volume-2.

[3]. T.E.Stirling : "Analysis of the design of two pumps using NEL methods" Centrifugal Pumps-Hydraulic Design-I Mech E Conference Publications 1982-11, C/183/82.

[4]. Numerical Calculation of the flow in a centrifugal blower impeller using Cartesian grid procedure of 2nd WSEAS int.Conference on applied and theoretical mechanics, Venice, Italy, November20-22,2006,According to john S.Anagnostopoulos.

[5]. Young-Kyun Kim, Tae-Gu Lee, Jin-Huek Hur, Sung-Jae Moon, and Jae-Heon Lee World Academy of Science, Engineering and Technology 50 2009.

[6]. International Journal of Rotating Machinery 2005:1, 45–522005 Hindawi Publishing Corporation Mechanical and Fluids Engineering Department, Southwest Research Institute, 6220 Culebra Road, an Antonio, TX 78238-5166, USA.

[7]. MA Xi-jin, ZHANG Huachuan, ZHANG Kewei. Numerical Simulation and Experiment Analysis of Thirdly Circulating Feed-water Mixed-flow Pump in Nuclear Power Station. FLUID MACHINERY. Vol.37, No.09, 2009 6-9.

[8]. Georgiana DUNCA1, Sebastian MUNTEAN 2, Eugen Constantin ISBĂŞOIU3, U.P.B. Sci. Bull., Series D, Vol. 72, Iss. 1, 2010.

[9]. Miner S.M. 2001, 3-D viscous flow analysis of a mixed flow pump impeller, International Journal of Rotating Machinery, Vol. 7, No. l, pp. 53-63.

[10]. Prepared for the33rd Joint Propulsion Conference and Exhibit cosponsored byAIAA**,** ASME, SAE, and ASEESeattle, Washington, July 6–9, 1997.

[11]. The 1997 ASME Fluids Engineering Division Summer MeetingFEDSM'97, June 22–26, 1997.